

Functional imaging of lung cancer using dual energy CT: how does iodine related attenuation correlate with standardized uptake value of 18FDG-PET-CT?

G. Schmid-Bindert · Thomas Henzler · T. Q. Chu · M. Meyer · J. W. Nance Jr ·
U. J. Schoepf · D. J. Dinter · P. Apfaltrer · R. Krissak · C. Manegold ·
S. O. Schoenberg · C. Fink

Received: 20 April 2011 / Revised: 10 June 2011 / Accepted: 27 June 2011 / Published online: 7 August 2011
© European Society of Radiology 2011

Abstract

Objectives To investigate the correlation between maximum standardized uptake value (SUV_{max}) of ^{18}F FDG PET-CT and iodine-related attenuation (IRA) of dual energy CT (DECT) of primary tumours and ^{18}F FDG PET-CT positive thoracic lymph nodes (LN) in patients with lung cancer.

Methods 37 patients with lung cancer (27 NSCLC, 10 SCLC, 86 ^{18}F FDG PET-CT positive thoracic LN) who underwent both ^{18}F FDG PET-CT and DECT were analyzed. The mean study interval between ^{18}F FDG PET-CT and DECT was ≤ 21 days in 17 patients. The mean and maximum IRA of DECT as well as of virtual unenhanced and virtual 120 kV images of DECT was analyzed and correlated to the SUV_{max} of ^{18}F FDG PET-CT in all tumours and ^{18}F FDG PET-CT positive thoracic lymph nodes. Further

subgroup analysis was performed for histological subtypes in all groups.

Results A moderate correlation was found between SUV_{max} and maximum IRA in all tumours ($n=37$; $r=0.507$; $p=0.025$) whereas only weak or no correlation were found between SUV_{max} and all other DECT measurements. A strong correlation was found in patients with study intervals ≤ 21 days ($n=17$; $r=0.768$; $p=0.017$). Analysis of histological subtypes of lung cancer showed a strong correlation between SUV_{max} and maximum IRA in the analysis of all patients with NSCLC ($r=0.785$; $p=0.001$) and in patients with NSCLC and study intervals ≤ 21 days ($r=0.876$; $p=0.024$).

Thoracic LN showed moderate correlation between SUV_{max} and maximum IRA in patients with study intervals ≤ 21 days ($r=0.654$; $p=0.010$) whereas a weak correlation was found between SUV_{max} and maximum IRA in patients with study intervals > 21 days ($r=0.299$; $p=0.035$).

Conclusions DECT could serve as a valuable functional imaging test for patients with NSCLC as the IRA of DECT correlates with SUV_{max} of ^{18}F FDG PET-CT.

Keywords Lung cancer · Dual energy computed tomography · ^{18}F FDG PET-CT · Tumor vascularity · Tumour staging

Introduction

^{18}F FDG PET and ^{18}F FDG PET-CT are considered superior to standard CT alone for the characterization of pulmonary nodules, evaluation of thoracic lymph nodes, planning of radiotherapy, and evaluation of therapeutic response in

G. Schmid-Bindert · T. Q. Chu · C. Manegold
Interdisciplinary Thoracic Oncology, Department of Surgery,
University Medical Center Mannheim,
Medical Faculty Mannheim, Heidelberg University,
Theodor-Kutzer-Ufer 1-3,
D-68167 Mannheim, Germany

T. Henzler (✉) · M. Meyer · J. W. Nance Jr · D. J. Dinter ·
P. Apfaltrer · R. Krissak · S. O. Schoenberg · C. Fink
Institute of Clinical Radiology and Nuclear Medicine,
University Medical Center Mannheim, Medical Faculty Mannheim,
Heidelberg University,
Heidelberg, Germany
e-mail: thomas.henzler@medma.uni-heidelberg.de

J. W. Nance Jr · U. J. Schoepf
Department of Radiology and Radiological Science,
Medical University of South Carolina,
Charleston, SC, USA

patients with lung cancer [1, 2]. Furthermore, several studies have indicated that the maximum standardized uptake value (SUV_{max}) of ^{18}F FDG-PET correlates with tumour aggressiveness and therefore has predictive value for patient outcome [3–10]. Miles et al. have already demonstrated that, in patients with lung cancer, the standardized perfusion value measured on dynamic contrast-enhanced CT (DCE-CT) strongly correlates with ^{18}F FDG uptake on PET [11].

Dual Energy CT (DECT) enables a selective visualization and quantification of the iodine-related attenuation (IRA) of intravenously injected iodinated contrast material and thus visualization and quantification of tumor blood supply at the time point of the data acquisition without the need of an additional unenhanced CT examination [12, 13]. In contrast to DCE-CT it can be performed routinely within a single breathhold and with similar radiation exposure. Assuming the distribution of iodine in tissue strongly correlates with local blood volume and vascular density, DECT may be used as a surrogate imaging test for the assessment of angiogenesis of tumours. Indeed, in a pilot study by Chae et al. pulmonary nodules could be differentiated by DECT as benign or malignant with a sensitivity of 92% [14].

The aim of this study was to evaluate the relationship between the IRA of DECT and the SUV_{max} of ^{18}F FDG PET-CT in patients with histologically confirmed lung cancer and PET-CT positive thoracic lymph nodes (LN).

Materials and methods

This study was approved by our institutional review board that waived informed consent for the retrospective data analysis of patients with histologically confirmed lung cancer who underwent both ^{18}F FDG-PET CT and DECT for a clinical indication at our institution.

Study population

Between July 2009 and July 2010, a total of 37 patients (29 men, 10 women; mean age 69 years (range 41–92 years) were identified and enrolled for data analysis (non-small cell lung cancer (NSCLC)=27; small-cell lung cancer (SCLC)=10); 86 ^{18}F FDG PET-CT positive thoracic LN. The mean time interval between ^{18}F FDG PET-CT and DECT was 27 ± 31 days (range 0 – 164 days) (Table 1).

To account for possibly confounding tumour changes between imaging exams, we divided our study population into two groups for subanalysis: The first group included 17 patients (NSCLC=13; SCLC=4; 63 LN) with a time interval of less than 21 days between ^{18}F FDG PET-CT and DECT examinations (9 ± 6 days; range 0–18 days) while the

Table 1 Patient characteristics

Characteristic	n (%)
Gender	
Male	29 (73.4%)
Female	8 (21.6%)
Histology	
NSCLC	27 (73%)
SCLC	10 (27%)
Stage NSCLC	
IIB	1 (2.7%)
IIIA	3 (8.1%)
IIIB	4 (10.8%)
IV	19 (51.4%)
Stage SCLC	
Limited	5 (13.5%)
Extensive	5 (13.5%)

second group included 20 patients (NSCLC=14; SCLC=6; 23 LN) with an interstudy interval >21 days (59 ± 31 days; range 23 – 164 days). We chose this interval considering treatment cycles are usually defined as 21 days; furthermore, recommendations for most clinical trials suggest intervals up to 28 days between initiation of treatment and the latest CT examination that will not be affected by significant changes in tumour size [15]. In some cases PET-CT and DECT were performed within an interval of less than 21 days. Reasons for this were the performance of a contrast-enhanced DECT in cases where the CT component of ^{18}F FDG PET-CT only consisted of a low-dose unenhanced CT performed for attenuation correction. Also in some cases PET-CT was performed for whole-body staging after a lung tumour was found on contrast-enhanced DECT.

CT imaging technique

All CT examinations were performed on a 64-channel dual source CT (SOMATOM Definition, Siemens Healthcare, Forchheim, Germany). Tube voltages were set to 140 kV (tube A) and 80 kV (tube B). To compensate for the lower photon output of tube B, the quality reference tube current of tube B was set to 235mAs, while tube A was operated with a quality reference tube current of 50mAs. The tube rotation time was 0.33 s. Automatic tube current modulation (CARE Dose 4D) was used in all patients. According to the manufacturer's recommendations, the detector collimation was set to 14 x 1.2 mm in order to minimize beam-hardening artifacts and improve the signal-to-noise ratio. All studies were performed after injection of 105 mL of iodinated contrast media (Iomeprol 400, Imeron 400, Bracco Imaging S.p.A., Milan, Italy) using a fixed delay before CT data acquisition of 35 seconds. The delay was chosen based on previous studies of dynamic contrast

enhanced MRI that have demonstrated that lung cancer typically shows peak enhancement 20–40 seconds after the start of the injection of contrast medium and a steady decrease of enhancement (i.e. wash-out) thereafter [16, 17]. Moreover, this delay resulted in typical late arterial phase images of the chest providing good visualization of the tumour, mediastinal and hilar lymph nodes, and thoracic vessels. A separate dataset for each tube kV as well as one linearly weighted average dataset (“virtual 120 kV,” using 70% tube A and 30% tube B) was calculated with a slice thickness of 2 mm and a reconstruction increment of 1.4 mm using a soft tissue kernel (D30f). Prior work has shown that using a linear blending algorithm combining 70% of the 140 kV data and 30% of the 80 kV data yields images with similar characteristics as a standard 120 kV single energy CT examination [12]. All CT data acquisitions were performed in a caudocranial direction during a mid-inspiratory breathhold.

¹⁸F-FDG-PET-CT protocol

All patients were examined on a clinical PET-CT system (Biograph mCT; Siemens Healthcare, Forchheim, Germany) with a 40-slice CT system. CT data was acquired using the following parameters: 12 x 1.2 mm detector collimation, pitch of 1.2, 300 ms gantry rotation time, 120 kV tube potential, and 30 mAs per rotation tube current time product. Axial images were reconstructed with a slice thickness of 3 mm and with an increment of 1.5 mm. If iodinated contrast material was indicated patients received 100 mL iomeprol 400 (Imeron 400, Bracco Imaging S.p.A., Milan, Italy) via an antecubital vein using a power injector (Stellant[®] D CT Injection System MEDRAD, INC, Warrendale, USA) at a flow rate of 2.5 mL/s. A saline chaser of 40 mL using the same flow rate followed all

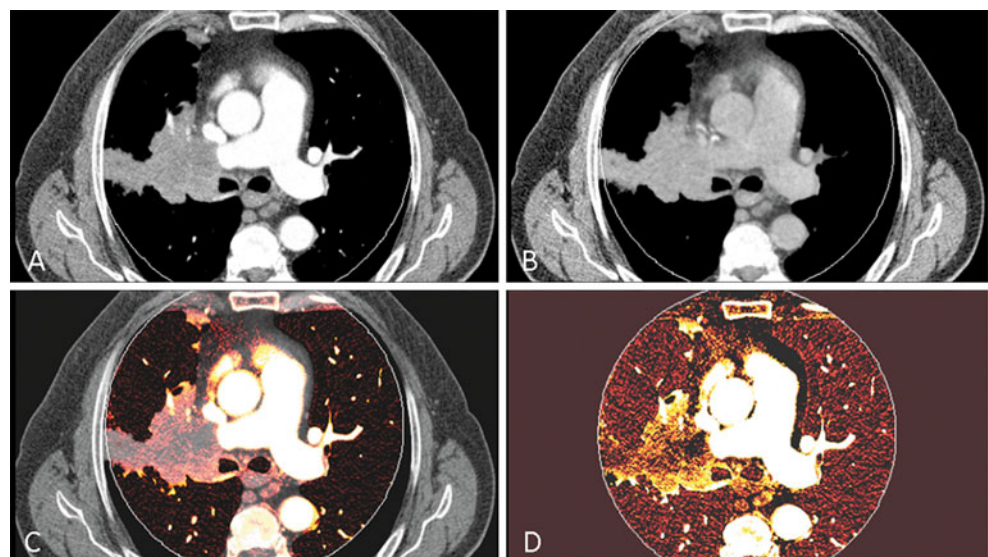
contrast injections. The delay before CT data acquisition was determined by bolus tracking in the ascending aorta using a dedicated software application (CARE dose, Siemens Healthcare, Forchheim, Germany).

PET data was acquired using the following parameters: in-plane spatial resolution of 5 mm and an axial field of view of 40 cm for each bed position. PET images were corrected for attenuation on the basis of the CT data and iterative reconstruction algorithms with three iterations and 24 subsets were performed (TrueX algorithm, Siemens Healthcare, Forchheim, Germany). PET imaging was performed 60 min after the administration of 5 MBq/kg of ¹⁸F-FDG. Patients had been instructed to fast for a minimum of 6 h before starting the examination. Blood samples collected before the injection of the radioactive tracer ensured blood glucose levels in the normal range (60–100 mg/dL).

Image analysis of DECT

DECT data analysis was performed in consensus by two experienced radiologists (C.F.T.H) with 12 and 4 years experience in chest CT. Datasets were transferred to a multi-modality workstation equipped with special software for the evaluation of DECT data (Dual Energy, VA21, Siemens Healthcare, Forchheim, Germany). We used a dedicated DECT algorithm (Liver VNC, Siemens Healthcare, Forchheim, Germany) that has been recommended for the evaluation of lung nodules in a previous study [14]. This algorithm calculates virtual non-contrast (VNC) images, images showing the IRA as well as virtual 120 kV images, calculated by linear blending of data from the 140 kV dataset 80 kV dataset using a weighting factor of 1:4 (Fig. 1). In each lesion the IRA, VNC and virtual 120 kV mean and maximum attenuation was measured within 3

Fig. 1 Axial contrast-enhanced DECT images of a 51 year-old man with histologically confirmed small cell lung cancer. **a** represents a 120 kV images, calculated by linear blending of data from the 140 kV dataset 80 kV dataset using a weighting factor of 1:4; **b** shows a calculated virtual non contrast image (VNC); **c** and **d** are calculated iodine related attenuation images in which the iodine distribution is color-coded



different regions of interest (ROIs) on the different image series. The mean value and standard deviation of the 3 different measurements was subsequently calculated and recorded. The size and location of the ROIs was kept constant between IRA, VNC, and virtual 120 kV series. To ensure that the same lesions at the same levels were measured on DECT and ^{18}F FDG PET-CT, the reports and the images of the PET-CT studies were available during data analysis on a separate workstation.

Image analysis of PET-CT

Image analysis was carried out by an attending radiologist board-certified in radiology and nuclear medicine (D.D) with more than 10 years experience in oncologic imaging. The primary tumour as well as the lymph nodes were evaluated by measuring the SUV_{max} . As usual, SUV_{max} was calculated as the ratio of the regional radioactivity concentration divided by the injected amount of radioactivity normalized to body weight using a ROI analysis. In detail, lung tumours and lymph nodes were analyzed by drawing an ellipsoid ROI including the entire tumour/lymph node and additionally a rim of approximately 1 cm. Lymph nodes were defined as malignant with an SUV_{max} of >2.5 according to Hellwig et al [18].

Statistical analysis

All statistical analyses were performed using SPSS 13.0 statistical package (SPSS Inc., Chicago, IL, USA). Continuous variables are expressed as mean \pm standard deviation, and categorical variables as the percentage frequencies and percentages. Pearson correlation was used to analyze the relationship between and SUV_{max} of ^{18}F FDG PET-CT and all measured CT values. A p value of <0.05 was considered to be statistically significant. Correlations were calculated for lung tumours and thoracic lymph nodes separately for group 1 and group 2 as well as for both groups together. Further subgroup analysis was performed for histological subtypes in all groups. Interpretation of correlation coefficient r was performed as followed: 0–0.1 no correlation; 0.2–0.4 weak correlation; 0.5–0.6 moderate correlation; 0.7–0.9 strong correlation; 1 perfect correlation.

Results

All SUV_{max} and DECT attenuation measurements are summarized in Table 2 for lung tumours and Table 3 for thoracic LN of all patients as well as for patients with an interstudy interval ≤ 21 days and those with an interstudy interval >21 days.

Table 2 Overview of attenuation and SUV_{max} measurements in lung tumours

	All patients				Patients with a interstudy interval <21 days (group 1)				Patients with a interstudy interval >21 days (group 1)						
	All tumors		NSCLC		SCLC		NSCLC		All tumors		NSCLC		SCLC		
	Mean	SD	Mean	SD	Mean	SD	Mean	SD	Mean	SD	Mean	SD	Mean	SD	
SUV_{max}	14.8 \pm 7.7		15.4 \pm 5.4		13.0 \pm 9.7		17.1 \pm 7.8		16.5 \pm 7.8		9.0 \pm 5.1		13.7 \pm 7.6		13.6 \pm 10.5
IRA mean	27.0 \pm 21.9		25.2 \pm 23.6		33.2 \pm 13.3		20.0 \pm 16.0		20.6 \pm 15.5		28.2 \pm 14.5		31.3 \pm 24.8		34.0 \pm 14.4
IRA max	74.7 \pm 32.3		76.4 \pm 34.4		68.4 \pm 24.7		81.9 \pm 35.5		80.7 \pm 34.3		66.0 \pm 24.7		70.6 \pm 31.2		68.8 \pm 27.1
VNC mean	39.9 \pm 12.5		41.5 \pm 11.6		38.9 \pm 14.6		41.5 \pm 11.6		37.1 \pm 10.5		21.3 \pm 30.7		45.8 \pm 19.3		50.2 \pm 19.2
VNC max	75.6 \pm 17.2		77.7 \pm 16.3		73.1 \pm 17.2		77.7 \pm 16.3		79.9 \pm 15.4		61.9 \pm 31.6		68.3 \pm 24.8		71.2 \pm 25.7
120 kV mean	66.7 \pm 31.8		69.4 \pm 31.0		65.2 \pm 34.0		61.1 \pm 29.1		59.4 \pm 26.2		58.7 \pm 24.9		77.1 \pm 36.7		80.1 \pm 31.7
120 kV max	148.7 \pm 49.8		153.0 \pm 49.7		144.5 \pm 51.3		163.3 \pm 45.7		161.4 \pm 44.2		149.5 \pm 37.4		143.9 \pm 54.5		149.9 \pm 54.5

Table 3 Overview of attenuation and SUV_{max} measurements in thoracic lymph nodes (LN)

	All patients				Patients with a interstudy interval <21 days (group 1)				Patients with a interstudy interval >21 days (group 1)							
	All LN		SCLC LN		All LN		NSCLC-LN		SCLC-LN		All LN		NSCLC-LN		SCLC-LN	
	Mean	SD	Mean	SD	Mean	SD	Mean	SD	Mean	SD	Mean	SD	Mean	SD	Mean	SD
SUV _{max}	8.0±5.4	8.4±5.6	5.9±3.7	7.9±5.8	8.2±6.1	6.6±4.1	8.3±4.4	9.2±4.3	4.0±0.9	35.5±18.0	33.6±25.0	65.4±28.7	21.5±30.0	63.1±25.7	54.3±49.4	128.2±61.2
IRA mean	32.9±19.7	33.8±20.8	28.9±13.6	32.5±18.3	33.8±19.3	26.5±11.7	34.0±23.6	33.6±25.0	35.5±18.0	65.0±21.1	66.3±22.5	58.7±11.4	65.5±18.7	66.6±20.0	60.4±9.7	63.4±27.0
IRA max	65.0±21.1	66.3±22.5	58.7±11.4	65.5±18.7	66.6±20.0	26.4±23.3	27.7±25.9	21.6±23.1	26.4±23.3	17.8±27.0	19.1±29.3	59.3±33.7	61.0±19.1	63.1±25.7	54.3±49.4	112.5±59.0
VNC mean	22.4±23.0	21.6±23.1	26.4±23.3	27.7±25.9	21.6±23.1	52.0±16.8	57.7±21.6	52.0±16.8	52.0±16.8	53.5±17.4	54.9±42.2	55.1±40.3	130.9±39.8	127.4±45.2	123.3±41.7	122.8±42.5
VNC max	53.5±17.4	52.0±16.8	61.0±19.1	57.7±21.6	52.0±16.8	55.5±39.4	59.9±45.9	55.5±39.4	55.5±39.4	54.9±42.2	55.1±40.3	130.9±39.8	127.4±45.2	123.3±41.7	122.8±42.5	122.8±42.5
120 kV mean	54.9±42.2	55.1±40.3	50.6±45.5	59.9±45.9	55.5±39.4	123.3±41.7	123.3±41.7	122.8±42.5	123.3±41.7	123.3±41.7	123.3±41.7	123.3±41.7	123.3±41.7	123.3±41.7	123.3±41.7	123.3±41.7
120 kV max	128.4±44.5	127.4±45.2	130.9±39.8	123.3±41.7	122.8±42.5	123.3±41.7	123.3±41.7	122.8±42.5	123.3±41.7	123.3±41.7	123.3±41.7	123.3±41.7	123.3±41.7	123.3±41.7	123.3±41.7	123.3±41.7

Lung tumours of all patients

Pearsons correlation analysis revealed a moderate correlation between SUV_{max} and maximum IRA ($r=0.507$; $p=0.025$) (Fig. 2a) when all lung tumours in this group were considered whereas only a weak correlation was found for mean IRA measurements ($r=0.376$; $p=0.0001$). No correlation was found between SUV_{max} and all other DECT attenuation measurements (Table 4). Subgroup analysis for histological subtypes showed a strong correlation between

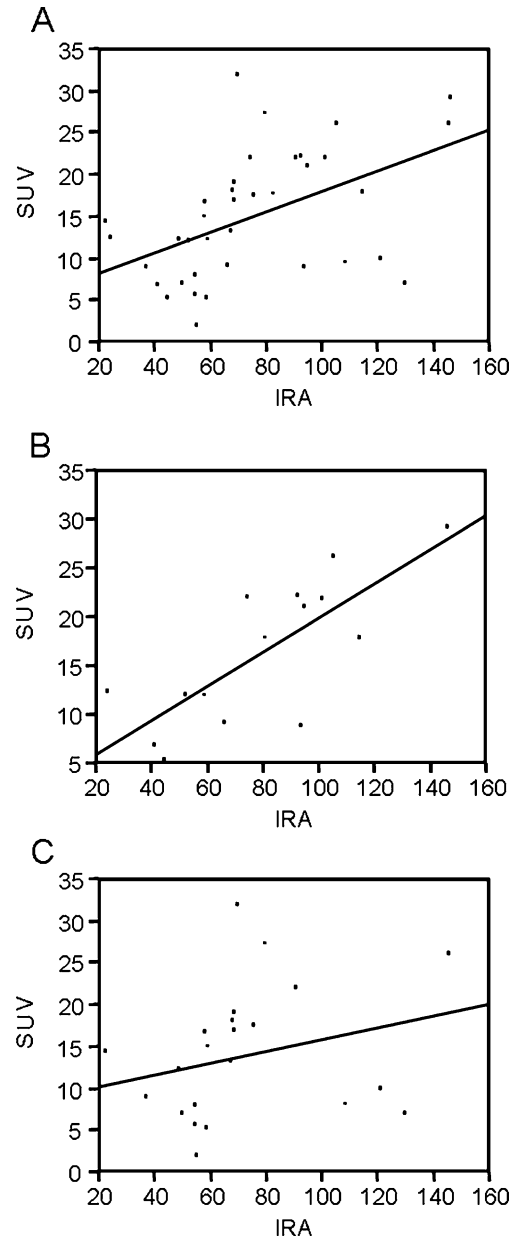


Fig. 2 Graph A shows the correlation between SUV_{max} and the iodine related attenuation (IRA) of the analysis that included all 37 tumours. Graph B and C show the correlation between SUV_{max} and the IRA in the analysis of the group that underwent both studies within 21 days (B) and in the group with a time interval >21 days (C)

Table 4 Summary of correlation coefficients between SUV_{max} and the different DECT attenuation measurements in lung tumors

	Patients with a interstudy interval <21 days (group 1)				Patients with a interstudy interval >21 days (group 2)				
	All tumors	NSCLC	SCLC	All tumors	All tumors	NSCLC	SCLC	SCLC	
IRA mean	0.376 (<i>p</i> =0.0001)	0.222 (<i>p</i> =0.028)	-0.021 (<i>p</i> =0.965)	0.395 (<i>p</i> =0.018)	0.409 (<i>p</i> =0.013)	0.127 (<i>p</i> =0.046)	0.129 (<i>p</i> =0.039)	0.198 (<i>p</i> =0.032)	0.099 (<i>p</i> =0.042)
IRA max	0.507 (<i>p</i> =0.025)	0.785 (<i>p</i> =0.001)	0.0151 (<i>p</i> =0.026)	0.768 (<i>p</i> =0.017)	0.876 (<i>p</i> =0.0001)	0.365 (<i>p</i> =0.044)	0.288 (<i>p</i> =0.024)	0.607 (<i>p</i> =0.032)	0.096 (<i>p</i> =0.081)
VNC mean	-0.119 (<i>p</i> =0.028)	-0.124 (<i>p</i> =0.042)	0.073 (<i>p</i> =0.044)	-0.039 (<i>p</i> =0.022)	-0.024 (<i>p</i> =0.04)	-0.103 (<i>p</i> =0.023)	-0.087 (<i>p</i> =0.035)	-0.021 (<i>p</i> =0.054)	-0.114 (<i>p</i> =0.039)
VNC max	0.122 (<i>p</i> =0.692)	0.001 (<i>p</i> =0.997)	0.161 (<i>p</i> =0.389)	0.122 (<i>p</i> =0.692)	0.0011 (<i>p</i> =0.997)	0.199 (<i>p</i> =0.512)	0.178 (<i>p</i> =0.489)	0.209 (<i>p</i> =0.463)	0.127 (<i>p</i> =0.701)
120 KV mean	0.145 (<i>p</i> =0.020)	0.085 (<i>p</i> =0.047)	0.142 (<i>p</i> =0.032)	0.111 (<i>p</i> =0.038)	0.156 (<i>p</i> =0.021)	0.078 (<i>p</i> =0.012)	0.173 (<i>p</i> =0.029)	0.179 (<i>p</i> =0.040)	0.112 (<i>p</i> =0.014)
120 kV max	0.043 (<i>p</i> =0.034)	-0.123 (<i>p</i> =0.031)	0.147 (<i>p</i> =0.035)	0.109 (<i>p</i> =0.043)	0.123 (<i>p</i> =0.038)	0.154 (<i>p</i> =0.036)	0.003 (<i>p</i> =0.019)	0.035 (<i>p</i> =0.011)	0.174 (<i>p</i> =0.041)

SUV_{max} and maximum IRA in NSCLCs ($r=0.785$; $p=0.001$) whereas no correlation was found in SCLC ($r=0.0151$; $p=0.026$). No correlation was found in the subgroup analysis of NSCLC and SCLC between SUV_{max} and all other DECT attenuation measurements (Table 4).

Lung tumours of patients with an interstudy interval between ¹⁸FDG PET-CT and DECT ≤ 21 days

A strong correlation was found between SUV_{max} and maximum IRA when all tumours in this group were considered ($r=0.768$; $p=0.017$) (Fig. 2b and 3) whereas there was only a weak correlation between SUV_{max} and mean IRA ($r=0.395$; $p=0.018$). Again, no correlation between SUV_{max} and all other DECT attenuation measurements was found (Table 4). In the subgroup analysis for histological subtypes the correlation between SUV_{max} and maximum IRA was strong in patients with NSCLC ($r=0.876$; $p=0.024$) whereas only a weak correlation was observed in patients with SCLC ($r=0.365$; $p=0.044$). Correlation between SUV_{max} and mean IRA was weak for patients with NSCLC ($r=0.409$; $p=0.013$) while no correlation was found for patients with SCLC ($r=0.127$; $p=0.046$). No correlation was found between SUV_{max} and all other DECT attenuation measurements neither for NSCLCs nor for SCLCs (Table 4).

Lung tumours of patients with an interstudy interval between ¹⁸FDG PET-CT and DECT >21 days

The correlation between SUV_{max} and maximum IRA was weak in patients with an interstudy interval of >21 when all tumours in this group were analyzed ($r=0.388$; $p=0.024$) (Fig. 4). All patients in this group received at least one treatment cycle between the two examinations. Correlation analysis between SUV_{max} and all other DECT attenuation values showed no correlations at all (Table 4). Subgroup analysis revealed a moderate correlation between SUV_{max} and maximum IRA for patients with NSCLC ($r=0.607$; $p=0.032$) but no correlation for patients with SCLC ($r=0.096$; $p=0.081$). Subgroup analysis between SUV_{max} and all other DECT attenuation values revealed no correlations (Table 4).

Thoracic lymph nodes of all patients

Considering all 86 PET-positive LN that have been included in this study we observed a moderate correlation between maximum IRA and SUV_{max} ($r=0.570$; $p=0.047$) (Fig. 5) whereas the correlation between SUV_{max} and the mean IRA was only weak ($r=0.263$; $p=0.036$). No correlation was found between SUV_{max} and all other DECT attenuation measurements in thoracic LN (Table 5). Subgroup analysis

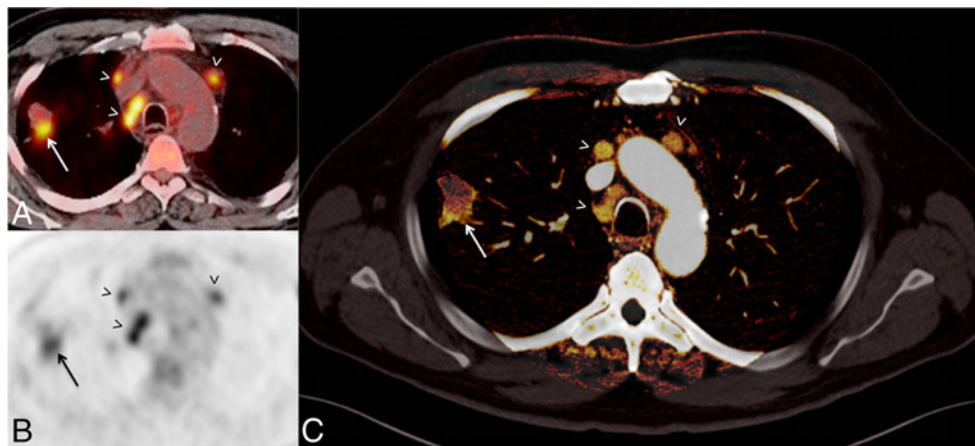


Fig. 3 Axial ^{18}F FDG PET-CT (**a**, **b**) and DECT (**c**) of a 65 year-old man with histologically confirmed non-small cell lung cancer who underwent both studies for initial tumour staging within 3 days prior to his first treatment. The dorsal portion of the tumour in the right

of LN showed a moderate correlation between SUV_{max} and maximum IRA ($r=0.694$; $p=0.038$) in patients with NSCLC whereas the correlation was weak in patients with SCLC ($r=0.341$; $p=0.031$).

Thoracic lymph nodes of patients with an interstudy interval between ^{18}F FDG PET-CT and DECT ≤ 21 days

A moderate correlation was found between SUV_{max} and maximum IRA when all LN in this group were considered ($r=0.654$; $p=0.010$). No correlation between SUV_{max} and all other DECT attenuation measurements was found in the analysis that included all LN of patients with an interstudy interval ≤ 21 days (Table 5).

upper lobe shows higher SUV_{max} and iodine related attenuation (IRA) values when compared to the ventral portion of the tumour (arrows in **a**, **b**, and **c**). All ^{18}F FDG PET-CT positive thoracic lymph nodes showed high IRA values in this patient (arrowheads in **a**, **b**, and **c**)

Histological subgroup analysis of LN in this group showed a strong correlation between SUV_{max} and maximum IRA in patients with NSCLC ($r=0.773$; $p=0.032$) whereas the correlation was still weak in patients with SCLC ($r=0.346$; $p=0.043$) (Fig. 5). No correlation was found between SUV_{max} and all other DECT attenuation measurements (Table 5).

Thoracic lymph nodes of patients with an interstudy interval between ^{18}F FDG PET-CT and DECT >21 days

Correlation analysis revealed only a weak correlation between SUV_{max} and maximum IRA for all LN that have been included in this group ($r=0.299$; $p=0.035$) as well as

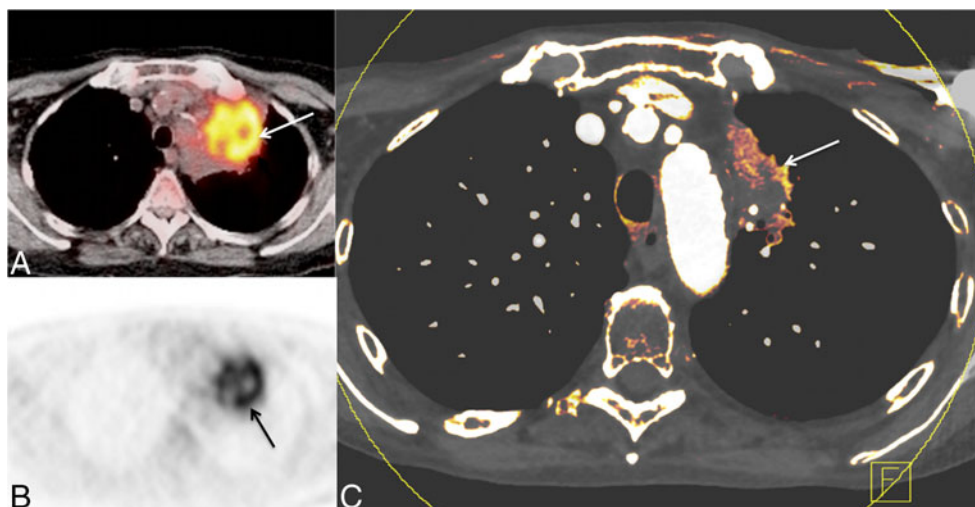
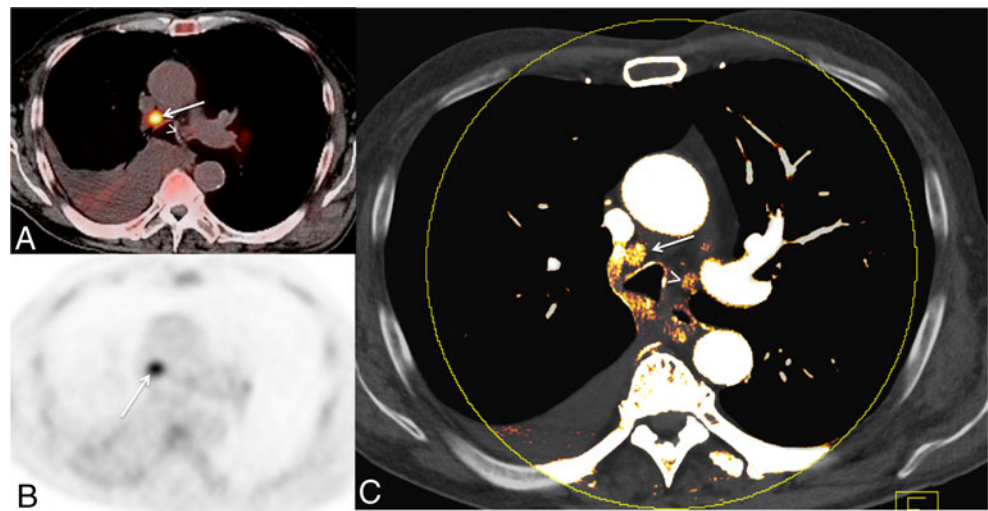


Fig. 4 Initial ^{18}F FDG PET-CT staging study (**a**, **b**) of a 72 year-old patient with histologically confirmed small cell lung cancer who underwent contrast-enhanced DECT (**c**) 43 days after the ^{18}F FDG PET-CT study and after 2 cycles of therapy. The upper portion of the tumour, which is shown on the cranial ^{18}F FDG PET-CT images, was

only residual at the date of the DECT study. The lower portion of the tumour that is shown on the DECT image shows no iodine related attenuation (IRA) in the center of the tumour due to central necrosis. The peripheral zone of the tumour still shows high IRA as a sign of tumour viability in this area (arrow in **c**)

Fig. 5 Axial ^{18}F FDG PET-CT (a, b) and contrast-enhanced DECT (c) of a 56 year-old women with histological confirmed non-small cell lung cancer who underwent both studies for initial tumour staging within 1 week. The ^{18}F FDG PET-CT positive lymph node adjacent to the azygos vein showed a high iodine related attenuation (IRA) (arrow in a, b, and c). The lymph node next to the left pulmonary artery showed high IRA but only a low SUV_{max} on ^{18}F FDG PET-CT (arrowheads in a, b, and c)



for the subgroup analysis of patients with PET positive LN but different histological subtypes (NSCLC=0.205; $p=0.013$; SCLC: 0.209; $p=0.037$). Again, no correlation between SUV_{max} and all other DECT attenuation measurements was found in the analysis of this group (Table 5).

Discussion

This study suggests that the maximum IRA of DECT correlates with the SUV_{max} of ^{18}F FDG PET-CT in histopathologically confirmed lung tumours and PET positive thoracic lymph nodes. The grade of correlation seems to be influenced by therapy since a much lower correlation was observed in patients with an interstudy interval of more than 21 days between both CT examinations. Furthermore, the correlation seems to be dependent on the histological subtypes as we found a strong correlation in patients with NSCLC but only a weak or no correlation in the various analyses of patients with SCLC.

Our findings are consistent with those observed by Miles et al., who investigated a potential correlation between the standardized perfusion value measured by DCE-CT and glucose metabolism measured by ^{18}F FDG-PET in patients with NSCLC. In this study, there was a positive correlation between SUV_{max} and the standardized perfusion value (SPV) [19], which is similar to our correlation between SUV_{max} and maximum IRA measurements using DECT. Although tumour perfusion and glucose metabolism are different physiologic processes, recent advances in tumour molecular genetics provide a biological rationale for an association between these two parameters. The p53 oncogene, which is frequently expressed in lung cancer, is known to promote both tumour angiogenesis [20] and glucose metabolism [21]. The increased microvessel density (MVD) that results from angiogenesis leads to increased tumour perfusion and thus iodine enhancement, whereas the

increased glucose metabolism produces increased ^{18}F FDG uptake in PET. These conceptual and biological relationships between tumour perfusion and ^{18}F FDG uptake are reflected in the correlation between maximum IRA and SUV_{max} in lung tumours and PET-positive thoracic lymph nodes found in the present study. With respect to this relationship, several studies have already correlated DCE-CT measurements to histological parameters of tumour angiogenesis, such as MVD or expression of VEGF [22]. Using DCE-CT, changes in perfusion and vascular permeability can be assessed based on analysis of time-density curves acquired with consecutive CT images obtained after injection of a bolus of iodinated contrast material [14, 23–28]. In patients with operable NSCLC, perfusion CT measurements of peak enhancement, blood flow, and relative blood volume have been shown to be significantly higher in VEGF-positive compared with VEGF-negative tumours [14, 29]. Peak enhancement, blood flow, and blood volume were also shown to correlate significantly with MVD [14, 29].

However, DCE-CT has several limitations that must be considered. First, with standard CT equipment, which has been used in the majority of studies, the sample volume of DCE-CT is restricted to a single or very limited number of transverse slices; this could be problematic for a quantitative assessment of angiogenesis in patients with multiple pulmonary nodules or large tumours. Although the capability to cover larger tissue volumes [12] and whole tumours [14] became feasible with the most recent multi-detector CT systems with broad detector arrays (up to 16 cm) or shuffle mode acquisitions, other limitations of DCE-CT have become more relevant, such as the considerable radiation dose to the patient. A typical effective dose for a volumetric whole-tumour technique for blood flow quantification in the lung with a temporal frequency of 1.5 seconds between helical acquisitions is 12mSV at 80 kV [30]. Moreover, post-processing and evaluation of tumour

Table 5 Summary of correlation coefficients between SUV_{max} and the different DECT attenuation measurements in thoracic lymph nodes

	All patients				Patients with a interstudy interval <21 days (group 1)				Patients with a interstudy interval >21 days (group 1)									
	NSCLC		SCLC		All tumors		NSCLC		SCLC		All tumors		NSCLC		SCLC			
	Correlation	p-value	Correlation	p-value	Correlation	p-value	Correlation	p-value	Correlation	p-value	Correlation	p-value	Correlation	p-value	Correlation	p-value		
IRA mean	0.263	(p=0.036)	0.081	(p=0.050)	-0.148	(p=0.020)	0.166	(p=0.019)	0.198	(p=0.015)	0.108	(p=0.021)	0.129	(p=0.029)	0.161	(p=0.027)	0.115	(p=0.041)
IRA max	0.570	(p=0.047)	0.694	(p=0.038)	0.341	(p=0.031)	0.654	(p=0.010)	0.773	(p=0.032)	0.346	(p=0.043)	0.299	(p=0.035)	0.205	(p=0.013)	0.209	(p=0.037)
VNC mean	0.173	(p=0.0001)	0.142	(p=0.0001)	0.054	(p=0.03)	0.063	(p=0.0001)	0.184	(p=0.0001)	0.148	(p=0.081)	0.078	(p=0.022)	0.089	(p=0.019)	0.102	(p=0.124)
VNC max	0.152	(p=0.005)	0.098	(p=0.007)	0.119	(p=0.010)	0.152	(p=0.0001)	0.161	(p=0.001)	0.019	(p=0.010)	0.126	(p=0.045)	0.091	(p=0.038)	0.178	(p=0.045)
120 KV mean	0.155	(p=0.028)	0.191	(p=0.019)	0.127	(p=0.031)	0.197	(p=0.024)	0.178	(p=0.018)	0.017	(p=0.028)	0.112	(p=0.033)	0.101	(p=0.041)	0.087	(p=0.036)
120 kV max	0.034	(p=0.023)	0.035	(p=0.043)	0.074	(p=0.015)	0.101	(p=0.035)	0.034	(p=0.043)	0.121	(p=0.042)	0.022	(p=0.038)	0.093	(p=0.020)	0.112	(p=0.012)

perfusion data is neither standardized nor generally available, which limits the integration of this technique into clinical routine. The main clinical benefit of a single acquisition DECT compared to a DCE-CT is that the whole tumour is covered within a single CT data acquisition and that the method is much less susceptible to respiratory motion since the data is acquired within a single acquisition during a single breathhold. Moreover, the patient’s radiation dose and total acquisition time will be much lower than with DCE-CT. In a feasibility study, Chae et al. evaluated the IRA of DECT for the differentiation of benign and malignant solitary pulmonary nodules and found a sensitivity, specificity, and accuracy of 92%, 70% and 82.2% when compared to histopathology [14]. However, until now no other studies have evaluated DECT in patients with lung cancer, emphasizing the need for larger studies to further evaluate the clinical usefulness of this technique.

Compared to the strong correlation between SUV_{max} and maximum IRA in patients with NSCLC, we only found a weak correlation in patients with SCLC. These differences could be explained by differences in tumour biology such as different angiogenetic properties between NSCLC and SCLC. It has been reported that ¹⁸F-FDG uptake is related to tumour angiogenesis and proliferative activity in NSCLC whereas this has not yet been reported for SCLC [31]. Our findings also indicate that the maximum IRA of DECT might be a useful surrogate parameter for the evaluation of therapy response, as it has been shown to correlate with the SUV_{max} of ¹⁸FDG PET-CT as well as with perfusion measurements on DCE-CT and DCE-MRI [32]. De Langen et al. demonstrated that patients with lung cancer showed lower SUV_{max} on ¹⁸FDG PET-CT and decreasing tumour perfusion on DCE-MRI after anti-angiogenic therapy when compared to their baseline imaging [32]; similarly, Lind et al. investigated the feasibility of DCE-CT in patients with advanced NSCLC who received anti-angiogenic and anti-EGFR treatment and found a significant decrease in tumour blood flow following targeted therapy. Moreover, early changes in tumour blood flow correlated with objective response and showed a trend towards longer progression free survival [33]. In another study involving 26 patients with stage III NSCLC, a significant decrease in the SUV_{max} of the primary tumour was found a few weeks after the completion of preoperative chemoradiotherapy when compared with the baseline study. Moreover, the sensitivity and specificity for differentiating residual tumours from pathologic complete responses by SUV_{max} criteria were both higher than those using a visual comparison (88% and 67% vs. 67% and 63%, respectively) [34].

Compared to the correlation values between ¹⁸FDG PET-CT and maximum IRA in patients with NSCLC, we

observed a lower correlation between SUV_{max} and the maximum IRA in thoracic lymph nodes. These findings can be explained either by differences in neoangiogenesis between intrapulmonary tumours and lymph node metastases or by the limited accuracy of both imaging tests to differentiate metastatic from reactive inflammatory lymph nodes. Furthermore, all lung tumours were confirmed to be malignant by histology while the classification of lymph nodes malignancy was based on ^{18}F FDG-uptake alone. It is well known that PET has only a moderate specificity and positive predictive value for determining the malignancy of lymph nodes in lung cancer since ^{18}F FDG is also taken up by inflammatory processes, and histological confirmation is required in cases where a curative intention to treat is being considered [35].

Our study has some potential limitations that must be considered. First, as this was a retrospective feasibility study, our patient population is relatively small, necessitating larger prospective studies for confirmation. Second, in contrast to the primary pulmonary tumours that have been included in this study, the malignancy of lymph nodes was not generally confirmed by histopathology. Third, we compared DECT attenuation measurements only to SUV_{max} measurements and not to other ^{18}F FDG PET-CT measurements like SUV_{mean} or histological parameters of tumour angiogenesis like MVD or VEGF. However, as this was a retrospective study further advanced histological analysis was not feasible. Moreover, it has recently been demonstrated that SUV_{max} measurements are more reliable and show less interobserver variability than SUV_{mean} measurements for staging as well as for the evaluation of therapeutic effects of chemotherapy or radiation therapy in patients with lung cancer [36]. Similarly to this, we believe that the correlations found between SUV_{max} and maximum IRA measurements but not between mean IRA and SUV_{max} could be based on the fact that maximum IRA values within a ROI are less affected by tumour heterogeneity than mean IRA values within the same ROI. Maximum IRA measurements within a ROI that includes necrotic hypoperfused areas adjacent to vital hyperperfused tumour tissue are not influenced by the proportion of different tissue viability within a ROI when compared to mean IRA measurements.

In conclusion, SUV_{max} and maximum IRA correlate well in patients with NSCLC and might be used as a supplement to ^{18}F FDG PET-CT for advanced tumour staging. Moreover, maximum IRA measurements could serve as a valuable functional imaging parameter for response evaluation.

Acknowledgement UJS is a consultant for and receives research support from Bayer-Schering, Bracco, General Electric, Medrad, and Siemens. The other authors have no conflict of interest to disclose. The study was approved by our Institutional Review Board and conducted in HIPAA compliance. Drs Henzler and Schmid-Bindert contributed equally to this study.

References

- Berghmans T, Dusart M, Paesmans M, Hossein-Foucher C, Buvat I, Castaigne C, Scherpereel A, Mascaux C, Moreau M, Roelandts M, Alard S, Meert AP, Patz EF Jr, Laffite JJ, Sculier JP (2008) Primary tumor standardized uptake value (SUV_{max}) measured on fluorodeoxyglucose positron emission tomography (FDG-PET) is of prognostic value for survival in non-small cell lung cancer (NSCLC): a systematic review and meta-analysis (MA) by the European Lung Cancer Working Party for the IASLC Lung Cancer Staging Project. *J Thorac Oncol* 3:6–12
- De Wever W, Ceyskens S, Mortelmans L, Stroobants S, Marchal G, Bogaert J, Verschakelen JA (2007) Additional value of PET-CT in the staging of lung cancer: comparison with CT alone, PET alone and visual correlation of PET and CT. *Eur Radiol* 17:23–32
- Orlacchio A, Schillaci O, Antonelli L, D'Urso S, Sergiacomi G, Nicoli P, Simonetti G (2007) Solitary pulmonary nodules: morphological and metabolic characterisation by FDG-PET-MDCT. *Radiol Med* 112:157–173
- Higashi K, Matsunari I, Ueda Y, Ikeda R, Guo J, Oguchi M, Tonami H, Yamamoto I (2003) Value of whole-body FDG PET in management of lung cancer. *Ann Nucl Med* 17:1–14
- Eschmann SM, Friedel G, Paulsen F, Reimold M, Hehr T, Budach W, Scheiderbauer J, Machulla HJ, Dittmann H, Vonthein R, Bares R (2006) Is standardised (^{18}F)FDG uptake value an outcome predictor in patients with stage III non-small cell lung cancer? *Eur J Nucl Med Mol Imaging* 33:263–269
- Higashi K, Ueda Y, Arisaka Y, Sakuma T, Nambu Y, Oguchi M, Seki H, Taki S, Tonami H, Yamamoto I (2002) ^{18}F -FDG uptake as a biologic prognostic factor for recurrence in patients with surgically resected non-small cell lung cancer. *J Nucl Med* 43:39–45
- Jeong HJ, Chung JK, Kim YK, Kim CY, Kim DG, Jeong JM, Lee DS, Jung HW, Lee MC (2002) Usefulness of whole-body (^{18}F)FDG PET in patients with suspected metastatic brain tumors. *J Nucl Med* 43:1432–1437
- Pandit N, Gonen M, Krug L, Larson SM (2003) Prognostic value of [^{18}F]FDG-PET imaging in small cell lung cancer. *Eur J Nucl Med Mol Imaging* 30:78–84
- Vansteenkiste JF, Mortelmans LA (1999) FDG-PET in the locoregional lymph node staging of non-small cell lung cancer. A comprehensive review of the leuven lung cancer group experience. *Clin Positron Imaging* 2:223–231
- Downey RJ, Akhurst T, Gonen M, Vincent A, Bains MS, Larson S, Rusch V (2004) Preoperative F-18 fluorodeoxyglucose-positron emission tomography maximal standardized uptake value predicts survival after lung cancer resection. *J Clin Oncol* 22:3255–3260
- Miles KA, Griffiths MR, Fuentes MA (2001) Standardized perfusion value: universal CT contrast enhancement scale that correlates with FDG PET in lung nodules. *Radiology* 220:548–553
- Johnson TR, Krauss B, Sedlmair M, Grasruck M, Bruder H, Morhard D, Fink C, Weckbach S, Lenhard M, Schmidt B, Flohr T, Reiser MF, Becker CR (2007) Material differentiation by dual energy CT: initial experience. *Eur Radiol* 17:1510–1517
- Pansini V, Remy-Jardin M, Faivre JB, Schmidt B, Dejardin-Bothelo A, Perez T, Delannoy V, Duhamel A, Remy J (2009) Assessment of lobar perfusion in smokers according to the presence and severity of emphysema: preliminary experience with dual-energy CT angiography. *Eur Radiol* 19:2834–2843
- Chae EJ, Song JW, Seo JB, Krauss B, Jang YM, Song KS (2008) Clinical utility of dual-energy CT in the evaluation of solitary pulmonary nodules: initial experience. *Radiology* 249:671–681
- Shanbhogue AK, Karnad AB, Prasad SR (2010) Tumor response evaluation in oncology: current update. *J Comput Assist Tomogr* 34:479–484

16. Schaefer JF, Schneider V, Vollmar J, Wehrmann M, Aebert H, Friedel G, Vonthein R, Schick F, Claussen CD (2006) Solitary pulmonary nodules: association between signal characteristics in dynamic contrast enhanced MRI and tumor angiogenesis. *Lung Cancer* 53:39–49
17. Schaefer JF, Vollmar J, Schick F, Vonthein R, Seemann MD, Aebert H, Dierkesmann R, Friedel G, Claussen CD (2004) Solitary pulmonary nodules: dynamic contrast-enhanced MR imaging–perfusion differences in malignant and benign lesions. *Radiology* 232:544–553
18. Hellwig D, Graeter TP, Ukena D, Groeschel A, Sybrecht GW, Schaefer HJ, Kirsch CM (2007) 18 F-FDG PET for mediastinal staging of lung cancer: which SUV threshold makes sense? *J Nucl Med* 48:1761–1766
19. Miles KA, Griffiths MR, Keith CJ (2006) Blood flow-metabolic relationships are dependent on tumour size in non-small cell lung cancer: a study using quantitative contrast-enhanced computer tomography and positron emission tomography. *Eur J Nucl Med Mol Imaging* 33:22–28
20. Kieser A, Weich HA, Brandner G, Marme D, Kolch W (1994) Mutant p53 potentiates protein kinase C induction of vascular endothelial growth factor expression. *Oncogene* 9:963–969
21. Mathupala SP, Rempel A, Pedersen PL (1997) Aberrant glycolytic metabolism of cancer cells: a remarkable coordination of genetic, transcriptional, post-translational, and mutational events that lead to a critical role for type II hexokinase. *J Bioenerg Biomembr* 29:339–343
22. Yi CA, Lee KS, Kim EA, Han J, Kim H, Kwon OJ, Jeong YJ, Kim S (2004) Solitary pulmonary nodules: dynamic enhanced multi-detector row CT study and comparison with vascular endothelial growth factor and microvessel density. *Radiology* 233:191–199
23. Charnley N, Donaldson S, Price P (2009) Imaging angiogenesis. *Methods Mol Biol* 467:25–51
24. Swensen SJ (2000) Functional CT: lung nodule evaluation. *Radiographics* 20:1178–1181
25. Swensen SJ, Brown LR, Colby TV, Weaver AL (1995) Pulmonary nodules: CT evaluation of enhancement with iodinated contrast material. *Radiology* 194:393–398
26. Swensen SJ, Morin RL, Schueler BA, Brown LR, Cortese DA, Pairolero PC, Brutinel WM (1992) Solitary pulmonary nodule: CT evaluation of enhancement with iodinated contrast material—preliminary report. *Radiology* 182:343–347
27. Yamashita K, Matsunobe S, Tsuda T, Nemoto T, Matsumoto K, Miki H, Konishi J (1995) Solitary pulmonary nodule: preliminary study of evaluation with incremental dynamic CT. *Radiology* 194:399–405
28. Zhang M, Kono M (1997) Solitary pulmonary nodules: evaluation of blood flow patterns with dynamic CT. *Radiology* 205:471–478
29. Tateishi U, Kusumoto M, Nishihara H, Nagashima K, Morikawa T, Moriyama N (2002) Contrast-enhanced dynamic computed tomography for the evaluation of tumor angiogenesis in patients with lung carcinoma. *Cancer* 95:835–842
30. Aukema TS, Kappers I, Olmos RA, Codrington HE, van Tinteren H, van Pel R, Klomp HM (2010) Is 18 F-FDG PET/CT useful for the early prediction of histopathologic response to neoadjuvant erlotinib in patients with non-small cell lung cancer? *J Nucl Med* 51:1344–1348
31. Kaira K, Oriuchi N, Shimizu K, Ishikita T, Higuchi T, Imai H, Yanagitani N, Sunaga N, Hisada T, Ishizuka T, Kanai Y, Endou H, Nakajima T, Endo K, Mori M (2009) Correlation of angiogenesis with 18 F-FMT and 18 F-FDG uptake in non-small cell lung cancer. *Cancer Sci* 100:753–758
32. de Langen AJ, van den Boogaart V, Lubberink M, Backes WH, Marcus JT, van Tinteren H, Pruijm J, Brans B, Leffers P, Dingemans AM, Smit EF, Groen HJ, Hoekstra OS (2010) Monitoring response to antiangiogenic therapy in non-small cell lung cancer using imaging markers derived from PET and dynamic contrast-enhanced MRI. *J Nucl Med* 52:48–55
33. Lind JS, Meijerink MR, Dingemans AM, van Kuijk C, Ollers MC, de Ruyscher D, Postmus PE, Smit EF (2010) Dynamic contrast-enhanced CT in patients treated with sorafenib and erlotinib for non-small cell lung cancer: a new method of monitoring treatment? *Eur Radiol* 20:2890–2898
34. Ryu JS, Choi NC, Fischman AJ, Lynch TJ, Mathisen DJ (2002) FDG-PET in staging and restaging non-small cell lung cancer after neoadjuvant chemoradiotherapy: correlation with histopathology. *Lung Cancer* 35:179–187
35. De Leyn P, Lardinois D, Van Schil PE, Rami-Porta R, Passlick B, Zielinski M, Waller DA, Lerut T, Weder W (2007) ESTS guidelines for preoperative lymph node staging for non-small cell lung cancer. *Eur J Cardiothorac Surg* 32:1–8
36. Huang YE, Chen CF, Huang YJ, Konda SD, Appelbaum DE, Pu Y (2010) Interobserver variability among measurements of the maximum and mean standardized uptake values on (18)F-FDG PET/CT and measurements of tumor size on diagnostic CT in patients with pulmonary tumors. *Acta Radiol* 51:782–788